The Effect of S-Layer Protein Adsorption and Crystallization on the Collective Motion of a Planar Lipid Bilayer Studied by Dynamic Light Scattering

Rainer Hirn,* Bernhard Schuster,# Uwe B. Sleytr,# and Thomas M. Bayerl*
*Universität Würzburg, Physikalisches Institut EP-5, 97074 Würzburg, Germany and #Center for Ultrastructure Research and Ludwig-Boltzmann-Institute for Molecular Nanotechnology, Universität für Bodenkultur Wien, A-1180 Vienna, Austria

ABSTRACT A dedicated dynamic light scattering (DLS) setup was employed to study the undulations of freely suspended planar lipid bilayers, the so-called black lipid membranes (BLM), over a previously inaccessible spread of frequencies (relaxation times ranging from 10^{-2} to 10^{-6} s) and wavevectors (250 $cm^{-1} < q <$ 38,000 cm^{-1}). For a BLM consisting of 1,2-dielaidoyl-*sn*-3-glycero-phosphocholine (DEPC) doped with two different proportions of the cationic lipid analog dioctadecyl-dimethylammonium bromide (DODAB) we observed an increase of the lateral tension of the membrane with the DODAB concentration. The experimentally determined dispersion behavior of the transverse shear mode was in excellent agreement with the theoretical predictions of a first-order hydrodynamic theory. The symmetric adsorption of the crystalline bacterial cell surface layer (S-layer) proteins from *Bacillus coagulans* E38-66 to a weakly cationic BLM (1.5 mol % DODAB) causes a drastic reduction of the membrane tension well beyond the previous DODAB-induced tension increase. The likely reason for this behavior is an increase of molecular order along the lipid chains by the protein and/or partial protein penetration into the lipid headgroup region. S-layer protein adsorption to a highly cationic BLM (14 mol % DODAB) shows after 7 h incubation time an even stronger decrease of the membrane tension by a factor of five, but additionally a significant increase of the (previously negligible) surface viscosity, again in excellent agreement with the hydrodynamic theory. Further incubation (24 h) shows a drastic increase of the membrane bending energy by three orders of magnitude as a result of a large-scale, two-dimensional recrystallization of the S-layer proteins at both sides of the BLM. The results demonstrate the potential of the method for the assessment of the different stages of protein adsorption and recrystallization at a membrane surface by measurements of the collective membrane modes and their analysis in terms of a hydrodynamic theory.

INTRODUCTION

Thermally excited undulations of membranes like the well-known flickering of red blood cells, observable with conventional light microscopy, is a phenomenon of functional importance for the cell, in particular for cell-cell and cell-surface interactions. Undulations or, more generally, collective membrane motions, are well-characterized both experimentally and theoretically in the low-frequency regime for cells (e.g., erythrocytes) and for large unilamellar vesicles (LUV) as membrane models (Helfrich and Servuss, 1984; Sackmann, 1996; Seifert and Langer, 1993). Their amplitude depends largely on the lateral tension of the membrane, and in general two regimes can be distinguished. The regime of negligible tension (e.g., LUV) where the membrane bending modulus dominates collective motions and the low-amplitude regime where the tension dominates all other membrane viscoelastic properties.

The methods used at low frequencies are based on microscopic interferometry (RICM) coupled with video data acquisition where the restricted bandwidth of the latter limits the access to motions with frequencies beyond 100 Hz (Sackmann, 1996; Zilker et al., 1987). Owing to this restriction, RICM is best suited for studying the low-frequency undulations that arise in tension-free systems.

However, there is a lack of data on collective motions in the mesoscopic- and high-frequency range, mainly due to the scarcity of suitable experimental methods. The only experimental proof of the existence of collective membrane motions in the high-frequency regime (upper GHz range) so far was obtained by coherent quasi-elastic neutron scattering (QENS) (Pfeiffer et al., 1993). In the mesoscopic range, solid-state NMR methods have been used to measure collective motions (Stohrer et al., 1991; Brown, 1996) but, as in the case of QENS, sensitivity problems and the need for using highly oriented samples pose severe restrictions for their application in biologically relevant systems. NMR has the additional disadvantage that it can detect time correlations, but no spatial ones, which constrains data analysis.

However, there exists a large body of theoretical work on collective membrane motions (Kramer, 1971; Fan, 1973; Helfrich and Servuss, 1984; Lipowsky, 1996; Seifert and Langer, 1993), which requires experimental methods selectively covering a wide range of frequencies (kHz–GHz) for validation. This disparity between available theoretical predictions and lacking experimental data underlines the need for new experimental approaches.

Dynamic light scattering (DLS) was suggested in the 1970s as a method to overcome many of the above limitations for studying collective motions of planar bilayers,

Received for publication 28 April 1999 and in final form 9 July 1999.
Address reprint requests to Prof. Thomas M. Bayerl, Universität Würzburg, Physikalisches Institut EP-5, Am Hubland, D-97074 Würzburg, Germany. Tel.: 49-931-888-5863; Fax: 49-931-888-5851; E-mail: bayerl@physik.uni-wuerzburg.de.

0006-3495/99/10/2066/09 $2.00

so-called black lipid membranes (BLMs; Crilly and Earnshaw, 1983a, b, 1985; Grabowski and Cowen, 1977) and soap films (Vrij et al., 1981). However, despite a good theoretical background (Kramer, 1971), the technical restrictions in the experimental layout did not allow the DLS technique to show its full potential for such studies, mainly due to a lack of sensitivity at higher frequencies. Theoretically, several membrane modes exhibit fluctuations of the dielectric tensor and thus can be expected to contribute to the DLS signal: 1) transverse shear (the motion of membrane constituents in normal direction to the interface) coupled with the splay mode describing the tilt motion of the long axis of anisotropic molecules, and 2) lateral compression (in-plane motion of the membrane constituents leading to fluctuations of the local density) coupled with the order fluctuation mode.

We have recently suggested a dedicated DLS experiment that overcomes the limitations of the past by a new setup design and improved sample preparation techniques. The new technique can cover a wavevector range from 250 to 38,000 cm^{-1} ($1.8 < \lambda < 250\ \mu m$) and a time scale of four orders of magnitude (from $6 \cdot 10^{-3}$ to $6 \cdot 10^{-7}$ s). With this setup we demonstrated for the first time that the subnanometer scale amplitudes of tension-dominated BLM undulations indeed show the theoretically predicted transition between a propagating and an over-damped regime, and can be described to a high precision by linear hydrodynamic theory (Hirn et al., 1999a,b). Moreover, the broad wavevector and time regime accessible by our DLS setup also allows new experiments on the effects of the coupling between proteins, peptides, or polymers and the membrane on collective membrane dynamics (Hirn et al., 1998b).

In this paper we concentrate on the modification of collective membrane motions due to the interaction of S-layer proteins with a BLM. The crystalline bacterial cell surface layer (S-layer) represents the outermost cell envelope component in organisms of almost every taxonomic group of walled Bacteria and Archaea (König, 1988; Sleytr et al., 1996a). They are in most cases composed of a single type of protein or glycoprotein with molecular weights ranging from 40 to 200, and they can exhibit oblique, square, or hexagonal lattice symmetry (Sleytr and Messner, 1989; Beveridge, 1994; Sleytr et al., 1996b). The S-layer from *Bacillus coagulans* E38-66 used in the present study is composed of identical, non-glycosylated protein subunits with a molecular weight of 100, and shows an oblique lattice symmetry with lattice parameters of $a = 9.4$ nm, $b = 7.4$ nm, and a base angle of $\gamma = 80°$. The crystalline protein layer with a thickness of ~5 nm shows pores of well-defined size and morphology with a diameter of 3.5 nm (Sára et al., 1992).

Isolated S-layer (glyco)protein subunits are endowed with the ability to assemble into monomolecular arrays at many different interfaces, including planar lipid monolayer (Pum et al., 1993; Wetzer et al., 1998; Schuster et al., 1998b; Weygand et al., 1999) and bilayer (Györvary et al., 1999; Schuster et al., 1998a). Electrostatic interactions between cationic charges in the membrane and anionic ones located in shallow pockets of the protein play a dominant role in the coupling and recrystallization of the proteins on lipid membranes (Wetzer et al., 1998; Sára and Sleytr, 1993). A comparison of the lipid monolayer structure before and after protein recrystallization shows minimal reorganization of the lipid chains but major rearrangements in the lipid headgroup region (Weygand et al., 1999). One can expect that the structural rearrangement is accompanied by significant alterations of the collective dynamics of the system, and thus of the micromechanical properties of this so-called "semifluid membrane" (Pum and Sleytr, 1994, 1996). The DLS technique allows for the first time the observation of the dynamic changes in the mesoscopic range at different stages of the S-layer recrystallization process. Moreover, the collective dynamic response of a bilayer to the attachment of the recrystallized S-layer can provide new clues about the detailed interaction mechanisms between the protein layer and the lipid membrane, as well as about the micromechanical properties of the S-layer itself.

THEORY

The undulation behavior of freely suspended planar membranes in solution was treated theoretically in terms of linear (i.e., Navier-Stokes) hydrodynamics by Kramer (1971). In this theory all interactions were treated as linear functions, and the anisotropic structure and dynamics of the lipid molecules owing to their partial ordering in the bilayer were ignored. For the special case of a membrane consisting of isotropic molecules symmetrically immersed in a homogeneous liquid it was concluded that the transverse shear mode is the only collective motion accessible by DLS on a physically meaningful time scale. All other modes are either completely insensitive to DLS or, like the lateral compression mode, exist at higher frequencies only (GHz range and higher) which are hardly resolvable. The transverse shear mode describes the out-of-plane motions of isotropic molecules. For the case of a BLM, this would correspond to the shearing between adjacent lipids in the direction of the membrane normal and leads to an effective fluctuation of the membrane area. The area fluctuation is opposed by the membrane tension arising from the interaction between the BLM forming lipids and the edge of the BLM bearing hole. This renders the collective BLM motion tension dominated and the dispersion relation of this transverse shear mode is given by:

$$2m\rho\omega^2 + \gamma q^3(q - m) = 0 \qquad (1)$$

where $m = (q^2 - i\rho\omega/\eta)^{0.5}$, $q = 2\pi/\lambda$ is the scattering vector, $\omega = \omega_0 - i\gamma$ is the complex frequency consisting of the eigenfrequency ω_0 and the damping constant γ, ρ and η are density and viscosity of the fluid, and $\gamma = \gamma_0 - i\omega\gamma'$ is a complex tension with the real part being the membrane tension and γ' the surface viscosity.

Fig. 1 shows a plot of ω_0 and γ versus q according to Eq. 1 using parameters typical for BLMs. A detailed discussion of this dispersion equation is given in Crilly and Earnshaw (1983b) and Kramer (1971).

For BLMs with tensions in the range $0.1 < \gamma_0 < 4$ mN/m, the left side of Fig. 1 describes an oscillating regime while the right one is characteristic of an over-damped regime. The crossover between the two regimes occurs fairly abruptly and is typically located around $q = 5000$ cm^{-1}. The damping constant γ_0 in the oscillating regime splits above the transition (bifurcation) point in two branches labeled γ_1 for the slower and γ_2 for the faster mode. For higher q-values the slower mode γ_1 asymptotes toward the limiting value $\xi = \gamma_0/\gamma'$. When the faster mode γ_2 assumes this value it merges into the bulk mode, which has the dispersion relation

$$i\omega - \eta q^2/\rho = 0 \tag{2}$$

and vanishes for ξ values above this limit. Because this bulk mode might couple to the fast undulation mode γ_2 it is likely that this thermally driven fast undulation mode dissipates its energy by this coupling. However, as the bulk mode is insensitive to DLS, a detection of γ_2 is unlikely.

So far, no DLS experiment was able to measure at sufficiently high q-values to cover this transition region, which would provide a critical testing of the still unverified Kramer theory. Equally important are measurements in the over-damped region where a clear dependence of γ_1 on γ' is predicted. By additionally considering the geometrical anisotropy of the lipids, Fan (1973) extended Kramer's theory by suggesting an additional splay mode coupled to Kramer's transverse shear mode with a coupling strength depending on the free energy variation arising from tilting the molecular director a lipid away from those of the adjacent lipids.

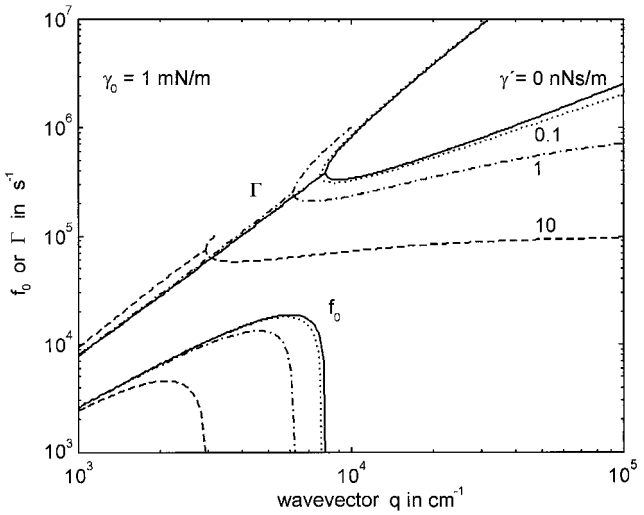

FIGURE 1 Theoretical dispersion curve of the transverse shear mode of a membrane according to Eq. 1, calculated for $\gamma_0 = 1$ mN/m, $\rho = 1$ mg/ml, and $\eta = 1$ m Pa s and at different surface viscosities γ': 0 nNs/m (—), 0.1 nNs/m (· · ·), 1 nNs/m (· - ·), and 10 nNs/m (- - -).

Thus, in Fan's treatment the membrane tension γ_0 is no longer a constant, but depends on the curvature energy κ and the undulation wavevector q, giving rise to an effective tension

$$\gamma_{0\text{eff}} = \gamma_0 + \kappa q^2. \tag{3}$$

Equation 3 shows that at high q-values, κ dominates the undulation behavior. However, for typical BLM parameters the κ-induced modifications of Eq. 1 would be non-negligible only at q-values well beyond the upper q-limit (35,000 cm^{-1}) of our DLS setup.

MATERIALS AND METHODS

Materials and membrane preparation

In all cases the BLM forming solution was 1% (w/v) lipid dissolved in n-decane. The n-decane 99+% (Sigma-Aldrich, Steinheim, Germany) was additionally purified using an alumina column until being completely colorless. The phospholipid 1,2-dielaidoyl-*sn*-3-glycero-phosphocholine (DEPC) and the positively charged amphiphile dioctadecyl-dimethylammonium bromide (DODAB) were purchased from Avanti Polar Lipids Inc. (Alabaster, AL) and used without further purification. The buffer used was Millipore water (resistance 18 MΩ) filtered through sterile 0.1-μm filter units (Millipore Corp., Bedford, MA) containing 2 mM $CaCl_2$ at pH 4.0 adjusted by citric acid and NaOH.

Isolation of S-layer subunits and recrystallization on lipid films

Growth of *B. coagulans* E38-66 in continuous culture, cell wall preparation, and extraction of S-layer protein with guanidine hydrochloride (GHCl, 5 M in 50 mM Tris/HCl buffer, pH 7.2, 20°C) were performed as previously described (Sleytr et al., 1996a). GHCl extracts were dialyzed after this procedure and the self-assembly products were sedimented for 20 min at 40,000 × *g* at 10°C. The clear supernatant containing the disassembled S-layer subunits or oligomeric precursors (~2 mg/ml solution) was used for all recrystallization experiments. In control experiments S-layer protein was recrystallized on a lipid monolayer of the same composition as the bilayer lipid membranes. The lipid monolayer was generated on a Langmuir film balance (611M, Nima, Coventry, UK) equipped with a Wilhelmy plate and a moveable barrier to adjust the surface pressure of the lipid monolayer to 26 ± 1 mN/m. Subsequently, the S-layer protein solution was injected beneath the lipid monolayer (final protein concentration 0.2 mg/ml buffer) and the recrystallization process was allowed to occur for 7 or 24 h, respectively. After this period of time the composite structure was transferred to carbon-coated electron microscope grids (Pum et al., 1993). For this purpose, the grids were deposited on the lipid film and removed in the horizontal orientation. The transferred protein/lipid structures were cross-linked with 2,5% glutaraldehyde (in 0.1 M sodium cacodylate buffer, pH = 7.2) for 20 min and stained with 2% uranyl acetate for 30 min. Transmission electron micrographs were taken with a Phillips CM12 TEM/STEM instrument (Phillips, Eindhoven, The Netherlands) operated at 80 kV. The quality of crystallization was determined by visual inspection. All recrystallization experiments were performed at room temperature (22 ± 1)°C.

BLMs of DEPC and of DEPC/DODAB mixtures (containing either 1.5 or 14 mol % DODAB) were prepared by gliding a Teflon loop carrying the BLM forming solution over a 3.5-mm diameter Teflon hole. The water level in the scattering cell was adjusted to 3 mm above the upper edge of the Teflon wall (see below), thus eliminating hydrostatic pressure differences. Before this the hole was pre-treated by spreading a methanol solution containing 2% (w/v) lipid on it, followed by solvent evaporation in air. After formation, the BLMs were allowed to equilibrate overnight before measurements commenced. By observing slow positional variations

of the reflected laser spot we established a slow relaxation of the BLM, which came to equilibrium ~8 h after its formation. After overnight equilibration and measuring this BLM in the protein-free state, the S-layer protein solution was added in equal amounts to both sides of the BLM using a microsyringe. The final protein concentration in the scattering cell was 0.2 mg/ml. DLS measurements were performed after 24-h equilibration of the protein with the BLMs for the case of the highly positively charged BLM (containing 14 mol % DODAB); an additional measurement was performed after 7 h equilibration.

Experimental setup

The BLM-containing scattering cell is a standard square glass cuvette of 40 × 10 × 10 mm (Hellma GmbH and Co., Mühlheim, Germany). A rectangular Teflon wall of 2 mm thickness having a hole of 4.5 mm in its center divides the cell diagonally into two compartments. Across this hole a 25-μm-thick Teflon foil with a 3.5 mm hole (the BLM bearing hole) is attached concentrically using a Teflon frame mount. We found that the use of the thin foil and the 3.5-mm-wide bearing hole provides the conditions required for having a widely planar and stable BLM allowing high q-resolution and eliminating any laser reflections from the Teflon. Moreover, the low thickness of the foil prevents positional fluctuations of the BLM as a whole, which would otherwise reduce the q-resolution. The long-time stability of the BLM (a typical membrane lasted for >2 days) was achieved by subjecting the foil to hole-drilling techniques that give a hole edge that appears perfectly smooth by light microscopy inspection.

Capillary waves of the water surface were eliminated by a suitable stopper in the upper part of the cell (≈1 cm above the BLM bearing Teflon hole) in direct contact with the water. The cuvette was mounted inside a water circulating system for controlling the cell temperature (22°C for all measurements) via a water bath thermostat (Neslab Instruments Inc., Portsmouth, NH).

The argon ion laser used (Innova 70–4 from Coherent Inc., Santa Clara, CA) was operated on its shortest line (457.9 nm, TEM_{00}) at 150 mW and the polarization of the beam was parallel to the membrane. The laser beam was focused on the BLM using a lens of 50 cm focal length to achieve a small angle of divergence (0.11°) and thus high q-resolution. The illuminated spot on the BLM (scattering area) had a diameter of 160 μm. The scattering geometry is shown in Fig. 2. The photomultiplier (PM) was mounted on a goniometer arm (PM and goniometer both from ALV GmbH, Langen, Germany) at an angle of 45° with respect to the BLM normal and at 30 cm distance from the scattering area. The q-regime of interest was selected by placing a pinhole (∅ 700 μm) near the BLM and a second one (∅ 80 μm) in front of the PM. For higher q-values ($q > 3400$ cm^{-1}) the 80-μm pinhole was replaced by a vertical slit aperture (200 × 2000 μm) to additionally collect the out-of-plane scattering intensity. The rationale for using a slit aperture has been discussed in detail elsewhere (Hirn et al., 1998b) and increases the signal-to-noise ratio of the detector signal by a factor of 80 without any reduction of signal quality.

The PM signal was pre-amplified and processed by autocorrelation in 388 channels using an ALV 3000 correlator (ALV GmbH, Langen, Germany). Measurements were done in the heterodyne mode using the diffuse scattering arising from the molecular roughness of the BLM as a local oscillator. The time increments used varied from 0.1 to 10 μs. The whole DLS setup was capsulated for dust protection and mounted on a 200-kg laser table (Melles-Griot, France) which was shock-insulated by four air-damping modules.

Data analysis

In the oscillating regime, the autocorrelation functions $G_o(t)$ were fitted to the theoretically expected function (Crilly and Earnshaw, 1983b)

$$G_o(t) = a + b\cos(\omega_0 t + \Phi)e^{-\Gamma_0 t} + ct \qquad (4)$$

where ct is the linear baseline correction and Φ is a phase factor. Corrections of $G_o(t)$ in the limit of small q to compensate for instrumental effects, as suggested in Crilly and Earnshaw (1983b) were not performed since these deviations from Eq. 4 were found completely negligible for $q > 400$ cm^{-1}. An example obtained for a BLM of pure DEPC is shown in Fig. 3.

At the transition point (bifurcation) between the oscillating and over-damped regime and its vicinity (±400 cm^{-1}), the data were fitted according to

$$G_t(t) = a + (b + ct)e^{-\Gamma_1 t} + dt \qquad (5)$$

This is the general expression for the asymptotic limit case of classical harmonic oscillators and indicates that in this transition region both over-damped modes γ_1 and γ_2 are detectable.

Finally, in the over-damped regime where two damping modes are predicted (Eq. 1), the data were fitted to

$$G_d(t) = a + be^{-\Gamma_1 t} + ce^{-\Gamma_2 t} + dt \qquad (6)$$

with a linear baseline correction dt.

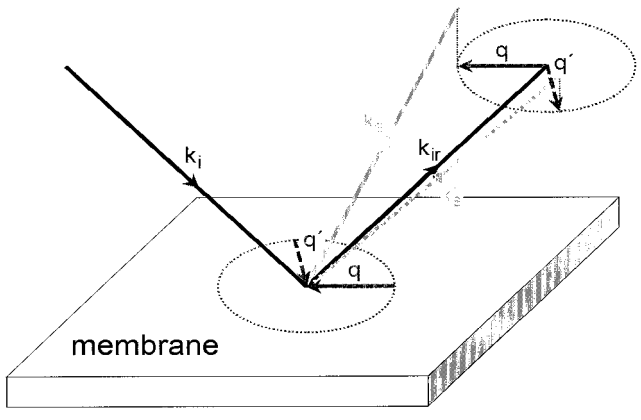

FIGURE 2 Schematic depiction of the scattering geometry used in our DLS setup for the detection, showing the incident vector k_i, the specular reflected vector k_{ir} (scattering angle 45°), the in-plane wavevector q, the in-plane scattered vector k_s, the out-of-plane wavevector q', and the out-of-plane scattered vector k_s'. Note that the modulus of the scattering vector remains approximately constant while its component along the membrane plane is changed by the vector q.

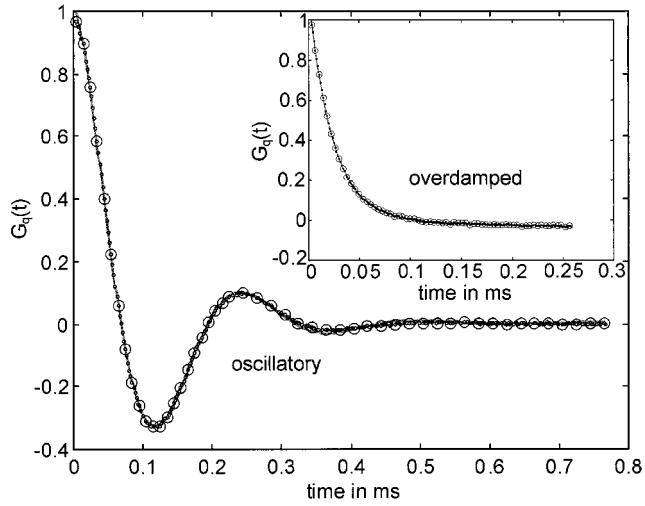

FIGURE 3 Example of correlation functions $G(t)$ of a DEPC-BLM obtained in the oscillating and in the over-damped regime (*inset*). Full lines represent fits according to Eq. 3. For clarity, some data points were omitted in the representation of the data (*circles*).

However, beyond the point where γ_2 assumes the value γ_0/γ', the fast mode disappears. For q-values beyond this point only the slow mode γ_1 was considered in the fitting procedure, as shown in Fig. 3.

Measuring autocorrelation functions with an S/N like that shown in Fig. 3 requires acquisition times between 30 s and 5 h depending on q and membrane tension. The latter is particularly important for high tensions since the amplitudes and thus the scattering intensity are reduced with increasing tension. Fitting the autocorrelation functions with the appropriate Eqs. 4, 5, or 6 provides the mode frequency f_0 and the damping constant γ.

The relationship between the q-value and the actual scattering angle φ adjusted with the goniometer is given by

$$q = n\frac{2\pi}{\lambda}\sqrt{(\sin(\Theta))^2 + (\sin(\Theta + \vartheta)^2 - 2\sin(\Theta)\sin(\Theta + \vartheta)} \quad (7)$$

where $n = 1.33$ is the refractive index of water, $\lambda = 457.9$ nm is the wavelength of the incident laser light, $\Theta = 45°$ is the static scattering angle, $\vartheta = \arcsin(\sin(\varphi)/n)$ is the corrected scattering angle (water/air interface), and φ is the variable the scattering angle.

RESULTS

Pure DEPC membranes

As a first experiment a pure DEPC membrane was measured at 22°C. Its complete dispersion curve in the range from 250 $cm^{-1} < q <$ 35,000 cm^{-1} is shown in Fig. 4. The data are compared with best fits (*solid lines*) according to Eq. 1. From that an average lateral tension $\gamma_0 = (0.42 \pm 0.03)$ mN/m and a negligible shear interfacial viscosity γ', acting in the normal direction of the membrane, is obtained. It is obvious that the agreement between experiment and theory is excellent over almost three orders of magnitude in q. The theoretically predicted transition from the damped to the over-damped case (cf. Fig. 1) is clearly observed experimentally at $q = 3300$ cm^{-1}. Minor deviations of $f_0(q)$ from the theory at lowest measurable q in Fig. 4 can be ascribed to a slight average overall equilibrium deformation of the BLM, giving rise to a diminished q-resolution in the low q-range. Moreover, at $q < 400$ cm^{-1} there could be a non-negligible contribution arising from the (Gaussian) instrumental function of the setup.

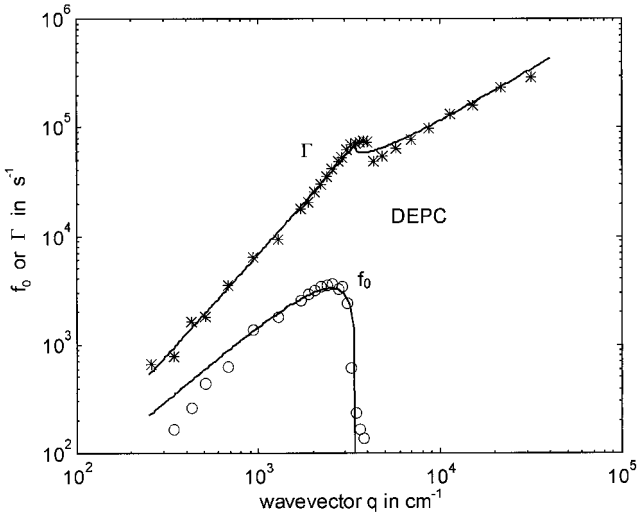

FIGURE 4 Mode frequency $f_0 = \omega_0/2\pi$ (*lower curve*) and damping constant γ (*upper curve*) versus mode wavevector q of a free planar bilayer (BLM) of DEPC, calculated from the autocorrelation functions measured at the corresponding q-values. The solid lines represent the Kramer theory (Eq. 1) fitted to the data, giving an average lateral tension $\gamma_0 = 0.42$ mN/m and a negligible surface viscosity γ'.

However, there is one striking discrepancy between theory and experiment observed in the over-damped regime (cf. Fig. 4): only one over-damped mode corresponding to the slow mode γ_1 can be fitted to the data, while theory additionally predicts a fast mode γ_2 (Fig. 1). The reasons for this discrepancy have been discussed in detail previously (Hirn et al., 1998b) and lie in the high probability that γ_2 merges with a DLS-insensitive bulk mode, rendering the relaxation of γ_2 too fast for being detectable beyond the vicinity of the bifurcation point.

Protein adsorption to weakly cationic BLMs without crystallization

It is well established that Coulomb forces are a dominant feature in the coupling of S-layer proteins to lipid bilayers (Wetzer et al., 1998; Pum and Sleytr, 1996). Recently it has been demonstrated that binding and recrystallization are optimized if cationic lipids are present in the surface layer (Wetzer et al., 1998). Following this observation, the coupling process to the BLM was facilitated by adding a cationic lipid component to the DEPC membrane. Therefore, the next step in our experiments was to study the undulation behavior of a BLM containing 1.5 mol % of the cationic amphiphile DODAB. Experiments using a monolayer of the same lipid composition at the air/water interface of a film balance showed that these conditions indeed facilitated S-layer protein coupling, but were insufficient to allow a crystallization of the proteins at the lipid surface. Therefore the DLS results will mainly reflect the dynamic changes induced by the Coulomb interaction between protein and BLM.

The results are shown in Fig. 5. A fit according to Eq. 1 gives a lateral tension of the DEPC/DODAB BLM of $\gamma_0 = (0.50 \pm 0.05)$ mN/m and again a negligible shear interfacial viscosity γ'. Thus, the lateral tension increases slightly by the DODAB addition compared to the pure DEPC BLM ($\gamma_0 = (0.42 \pm 0.03)$ mN/m) shown in Fig. 4. Moreover, the presence of DODAB reduced the (local) planarity of the BLM. This was clearly observed by a slightly increased fuzziness of the outer edges of the specular reflected laser spot. For this reason, no q-values below 1000 cm^{-1} are shown in Fig. 5.

Despite the reduction in data quality in the low-q range, there is still a remarkable agreement between theory and experiment over the wide q-range covered by the DLS measurement. This indicates that the DODAB-doped BLM continues to be tension-dominated and that there is no indication of any influence of the membrane bending energy κ.

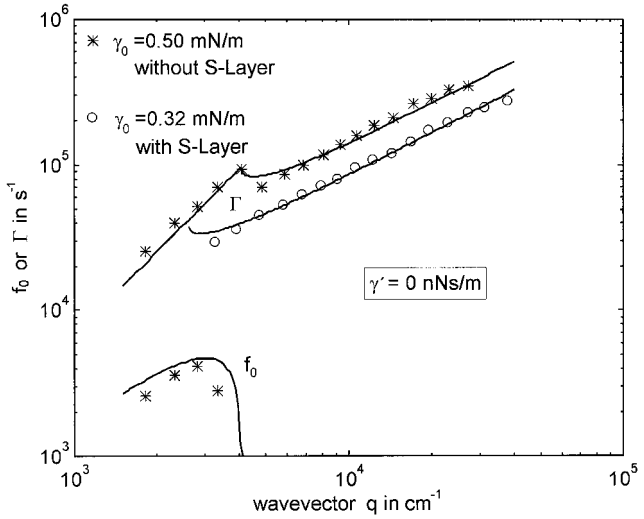

FIGURE 5 Mode frequencies f_0 and damping constants γ versus mode wavevector q of a DEPC-BLM doped with 1.5 mol % DODAB (∗) and the same membrane after the adsorption of S-layer protein at both sides of the bilayer (○). The solid lines represent fits to the data according to Eq. 1, giving an average lateral tension $\gamma_0 = 0.50$ mN/m before and $\gamma_0 = 0.32$ mN/m after the protein adsorption. In both cases the surface viscosity γ' was negligible. Note that after the protein adsorption no oscillation of the autocorrelation function was detectable in the range for $q > 1100$ cm^{-1}.

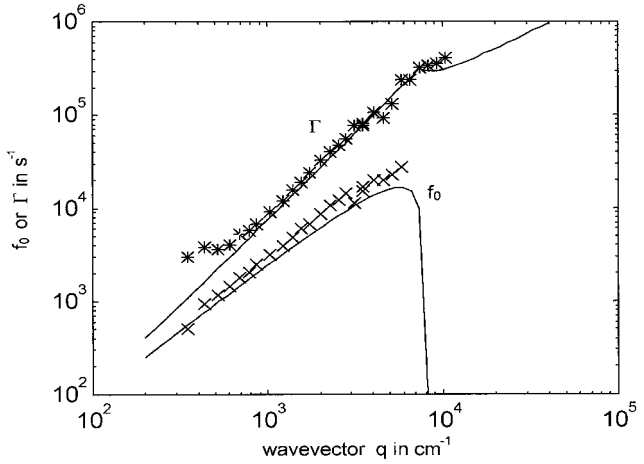

FIGURE 6 Mode frequency f_0 (×) and damping constants γ (∗) versus mode wavevector q of a DEPC-BLM doped with a high DODAB concentration (14 mol %). The solid lines represent fits to the data according to Eq. 1, giving a lateral tension $\gamma_0 = 0.91$ mN/m and a negligible surface viscosity γ'.

The addition of the S-layer proteins and incubation for 24 h has a remarkable effect on the collective BLM dynamics. The bifurcation point is shifted to lower q-values to such an extent that no oscillations of the BLM were detectable. Thus the system S-layer/BLM is over-damped over a wide q-range starting at q-values above 1200 cm^{-1}. Fitting Eq. 1 to the data now gives $\gamma_0 = (0.32 \pm 0.03)$ mN/m, while the shear interfacial viscosity γ' remains negligible.

It should be noted that the DODAB-doped BLM in absence of the proteins did not show any changes after 24 h, as was confirmed by a control experiment. Thus, the coupling of S-layer proteins to the DODAB-doped BLM caused a reduction in its lateral tension by 40%, rendering the system over-damped over the DLS-accessible q-range.

Crystalline S-layers at strongly cationic BLMs

In a third series of DLS experiments, we have used a significantly higher positive surface charge of the BLM to induce not only S-layer protein adsorption, but also its recrystallization into monomolecular arrays. Transmission electron microscopy (TEM) inspection of monolayers of DEPC containing 14 mol % DODAB transferred from a film balance showed partial crystallization after 7 h, and nearly complete crystallization into coherent lattices after 24-h incubation with S-layer proteins dissolved in the buffer.

The dispersion curve of a BLM of this lipid composition before the addition of the protein is shown in Fig. 6. The tendency of the cationic lipid to increase the lateral tension, which was already indicated by the measurement at 1.5 mol % DODAB, became quite obvious at this high DODAB proportion. The fit according to Eq. 1 gave a lateral tension $\gamma_0 = 0.91 \pm 0.06$ mN/m, more than twice the value measured for the pure DEPC-BLM.

The addition of the protein caused further drastic dynamic changes of the membrane that were measured after two incubation times: 7 h and 24 h. The (electrostatic) coupling of the protein within the 7-h incubation period caused a further increase of the fuzziness of the specular reflected laser spot edges, indicating a loss of planarity that prohibited DLS measurements at low q-values (Fig. 7). Fitting Eq. 1, we now observed a drastic reduction of the tension by the protein adsorption down to 0.15 ± 0.02 mN/m, which allowed us to measure the slow over-damped mode over the q-range comparable to that for the pure DEPC-BLM. Interestingly, the dispersion curve now showed a significant deviation from the theoretical behavior expected for negligible surface viscosity γ': the over-damped mode exhibited a systematic down-bend toward the q-axis for increasing q-values. This is exactly the behavior expected by the theory (Eq. 1) for the case of a non-zero surface viscosity γ' (cf. Fig. 1). Indeed, the fit to the data shown in Fig. 7 *A* using a complex surface tension gives not only the above-mentioned low tension of $\gamma_0 = 0.15$ mN/m, but also a non-negligible surface viscosity γ' of 5.0 nNs/m. After 24-h incubation of the same sample, we observed a dispersion behavior that still showed the bending indicative for non-zero surface viscosity in the lower q part of the over-damped regime, but which additionally exhibited an exponential-like increase at highest q-values (Fig. 7 *B*).

This latter behavior is not covered anymore by the Kramer theory, but it has been predicted in Fan's modification of this theory, where the effect of membrane bending energy κ to the dispersion behavior at high q was explicitly considered. Therefore, the fit according to Eq. 3 shown in Fig. 7 *B* for the case of 24-h incubation now considers three

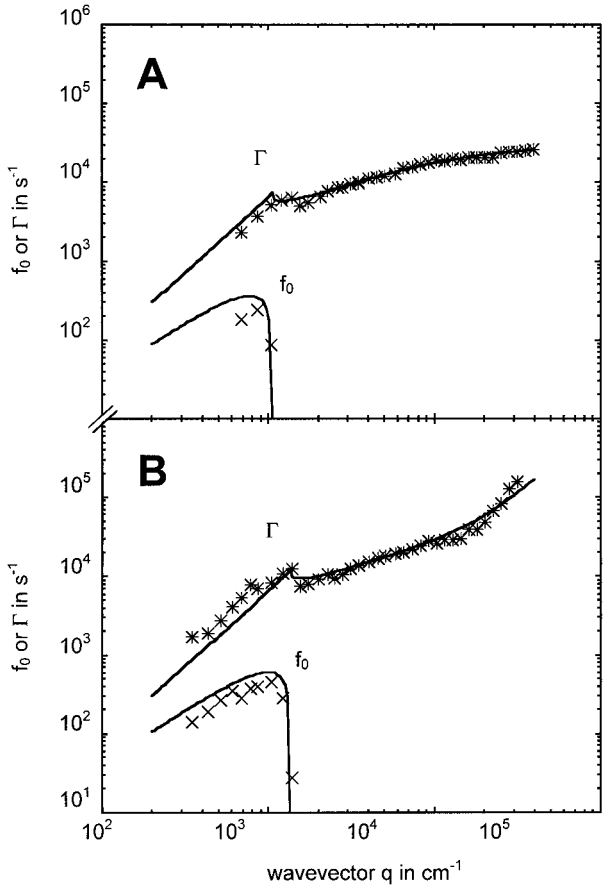

FIGURE 7 Same sample as shown in Fig. 6, but after the adsorption of S-layer proteins at both sides of the strongly cationic BLM after 7-h (*A*) and 24-h (*B*) incubation. The solid lines represent fits to the data according to Eq. 1 (*A*) and Eq. 3 (*B*). In both cases γ' is no longer negligible ($\gamma' = 5.0$ nNs/m), and for the 24-h incubation (*B*) a bending energy of $\kappa \approx 5 \cdot 10^{-17}$ J was obtained.

parameters: tension γ_0, surface viscosity γ', and bending κ. We obtain values of $\gamma_0 = 0.2$ mN/m and $\gamma' = 5.0$ nNs/m similar to those obtained after 7 h incubation, but additionally a bending energy $\kappa = 5\ 10^{-17}$ J. Although providing a qualitatively correct description of the data in the highest q regime, the quality of the fit at high q is clearly not satisfactory because the data increase is steeper than that of the fit function. However, considering that the errors of the DLS measurements for highest q-values due to limited S/N are rather large, we have put more weight to a good fit at low and intermediate q-values. Thus the absolute value of κ obtained by this procedure must be taken with caution and should reflect only the order of magnitude of bending energy. The results of the data analysis are summarized for all BLM systems studied in Table 1.

DISCUSSION

The data shown in Figs. 4–7 characterize the viscoelastic dispersion behavior of the transverse shear mode of a BLM over an exceedingly wide q-range. For comparison, previously reported DLS measurements on BLMs (Crilly and Earnshaw, 1983b) were limited to $q_{max} \sim 1800$ cm^{-1}, while for the present work we have $q_{max} \sim 38{,}000$ cm^{-1}. This allowed the experimental observation of transitions between the oscillatory and the over-damped regime of the transverse shear mode, in excellent agreement with the theoretical predictions (Eq. 1), thus providing strong support for the validity of this linear hydrodynamic theory. The results obtained in this work can be considered as reflecting different stages of the association between the protein and the BLM, controlled by the BLM surface charge and incubation time.

TABLE 1 Summary of the data analysis for all BLMs studied in terms of the parameters lateral tension γ_0, surface viscosity γ', and bending energy κ

BLM	γ_0 (mN/m)	γ' (nNs/m)	κ (J)
DEPC	0.42 ± 0.03	≈0	—
DEPC/DODAB (1.5 mol %)	0.50 ± 0.05	≈0	—
+ S-layer protein @ 24 h incubation	0.32 ± 0.03	≈0	—
DEPC/DODAB (14 mol %)	0.91 ± 0.06	≈0	—
+ S-layer protein @ 7 h incubation	0.15 ± 0.02	5.0 ± 0.5	—
+ S-layer protein @ 24 h incubation	0.20 ± 0.02	5.0 ± 0.8	$5 \cdot 10^{-17}$

The errors given were estimated from the mean squared residuals of the data fits. The error of κ is within one order of magnitude.

Effect of cationic lipids on transverse shear motion

Before we enter the discussion of these effects, some consideration of the effects of the cationic lipid DODAB on the collective BLM motion is justified. The presence of DODAB causes an increase of the lateral tension by more than a factor of two compared to the pure DEPC BLM (Fig. 6) and thus a corresponding reduction in amplitude of the transversal shear motion. Three processes may provide major contributions to this behavior. 1) The modification of the Stern layer by the cationic DODAB will result in a higher counterion density in the vicinity of the lipid headgroups that may reduce the transverse shear motion. 2) The presence of cationic lipids causes the choline headgroups to align their P-N dipole toward a more parallel orientation with respect to the membrane normal (MacDonald et al., 1991). The choline headgroup in its undisturbed conformation (P-N dipole perpendicular to the membrane normal (Büldt et al., 1978)) dominates the molecular area. Thus, this change of orientation leading to a reduced molecular headgroup area may increase the steric interaction between the hydrophobic chains. As a result, the molecular frictional drag for transverse shear between adjacent lipids will increase, and could reduce the amplitude of this collective motion. 3) The DODAB chains are presumably in an all-*trans* conformation (chain melting temperature of pure DODAB is 54°C (Linseisen et al., 1996)) while the DEPC

chains are fluid at room temperature. It is conceivable that the resulting complex mixing between the two components contributes to an increased friction for transverse shear motion. To establish which of the above-discussed mechanisms dominates the observed increase of BLM tension would require systematic studies as a function of ionic strength of the buffer and chain length of the cationic lipid component.

Protein adsorption and two-dimensional crystallization at cationic BLMs

A striking experimental result is the protein-induced reduction of the lateral tension down to 62% of its initial value (1.5 mol % DODAB) and to 17% of its initial value (14 mol % DODAB). This is the opposite behavior to what we observed previously for the binding of a streptavidin layer to a (zwitterionic) DEPC BLM via biotinylated lipids, where an increase in γ_0 by a factor of three was observed (Hirn et al., 1998b). This indicates significant differences in the interaction mechanism between membrane and protein studied in the present work. The most significant difference is certainly the well-established dominance of Coulomb interaction in the process of S-layer protein adsorption and crystallization (Pum and Sleytr, 1996). Furthermore, recent x-ray reflectivity work on S-layers crystallized to lipid monolayers suggests that amino acid side chains of the proteins may insert into the headgroup region of a zwitterionic phospholipid monolayer and that the crystalline protein layer can alter the lipid headgroup orientation (Weygand et al., 1999).

The partial penetration of the protein into the headgroup region will cause a dehydration of the lipid headgroups, which in turn may force the lipid chains into a state of higher molecular order (Diederich et al., 1996). This higher order may provide a major contribution to the observed lowering of tension. We tested the surmise of a facilitation of transverse shear with increasing molecular order of the chains by measuring the dispersion curve of a pure DEPC-BLM (Fig. 4) at different temperatures. Indeed, the measurements at 50°C (after heating up the BLM from 22°C) gave a lateral tension which was about twice that of the above-reported value of $\gamma_0 = 0.42$ mN/m. This result strongly suggests that increasing chain disorder is a hindrance for transverse shear of the DEPC molecules. The experimental observation that the S-layer formation causes the BLM to become less planar is a strong indication that partial penetration occurs.

A second mechanism that is likely to contribute to the lowering of γ_0 is a possible protein-induced lateral segregation of the cationic DODAB molecules. DODAB may become enriched at sites where the inner face of the adsorbed protein exhibits an excess of opposite charges (Fig. 6). Since DODAB is in an all-*trans* state at room temperature, one can conceive the BLM after the protein adsorption as being composed of lateral immobilized, pillar-like DODAB clusters surrounded by a large excess of fluid-like, highly mobile DEPC. The presence of the rigid DODAB pillars may contribute to a synchronization of the transverse shear motions in the two opposite, DODAB-depleted monolayers and thus give rise to higher amplitudes (and consequently lower tension) in comparison with the BLM before the protein adsorption.

Another very interesting result is the occurrence of a non-negligible surface viscosity γ' under conditions of protein adsorption at a strongly cationic BLM after 7 h incubation time. It indicates that the crowding of the proteins at both BLM surfaces by Coulomb attraction must change the local hydrodynamics in a way that the water flow connected with the transverse shear motion dissipates significantly more energy. It is conceivable that microcrystals of the protein have already been formed at the strongly cationic BLM after 7 h incubation time (Fig. 7), which would strongly oppose the water flow and additionally alter the lipid hydration in the vicinity of the BLM surface.

However, our finding that the surface viscosity γ' is negligible for plain BLMs (Fig. 5) and for the weakly cationic BLM with proteins (Fig. 6) is not surprising. The low amount of solvent (decane) resting inside the BLM simply acts as a lubricant for motions involved in the transverse shear process and leads to an effective decoupling between the two monolayers.

Large-scale two-dimensional crystallization after 24-h incubation of the protein, resulting in a tight S-layer symmetrically bound to the BLM (Fig. 7 *B*), does not significantly change the complex tension γ, but renders the BLM extremely stiff, i.e., drastically increases its bending modulus. This allowed us to observe for the first time the effect of a non-negligible bending energy κ for this special case, which is shown by the exponential-like increase of the dispersion curve at highest q-values. For a plain BLM like that of DEPC shown in Fig. 4, the value of κ is so low that an observation of this behavior would require measurements over a q-range of up to 10^5 cm^{-1} (Hirn et al., 1999a; Fan, 1973). The fit to the data after 24-h incubation (Fig. 7 *B*) shows that the general behavior of the dispersion curve for non-negligible κ at high q is (at least qualitatively) well-described by the theoretical prediction (Eq. 3) for this special case. The value of $\kappa = 5 \times 10^{-17}$ J provided by the fit is about three orders of magnitude higher than observed for erythrocyte or vesicular membranes, and is in the same order as that of polyethylene (Sackmann, 1996). This tremendous increase of κ by the S-layer formation does not directly reflect the bending stiffness of the two-dimensionally crystallized S-layer, but rather that of a composite structure consisting of two S-layers strongly coupled to a cationic BLM sandwiched between the two S-layers. This composite structure may exhibit a significantly higher κ than the single S-layers.

CONCLUSIONS

The DLS method is a sensitive tool used to detect the alterations of BLM collective motions caused by the ad-

sorption and two-dimensional crystallization of a protein layer over wide and previously inaccessible ranges in wavevector and frequency. The method can clearly distinguish between protein adsorption, as in the case of a weakly cationic BLM, from a S-layer recrystallization at the strongly cationic membrane. For the latter case, the technique indicates that in the course of the crystallization process the surface viscosity increases first; at a later stage the membrane bending stiffness becomes sufficiently high so that the bending energy dominates the dispersion curve at high q-values. This shows the potential of the DLS technique for monitoring the dynamic and viscoelastic changes in the course of protein recrystallization at a model membrane.

The expert help of Markus Hildenbrand in some DLS measurements and in data analysis is gratefully acknowledged.

This work was supported by grants from the Deutsche Forschungsgemeinschaft, from the Austrian Science Foundation, Project S7205 (U.B.S.) and the Austrian Ministry of Science and Transportation.

REFERENCES

Beveridge, T. J. 1994. Bacterial S-layers. *Curr. Opin. Struct. Biol.* 4:202–212.

Brown, M. F. 1996. Membrane structure and dynamics studied with NMR spectroscopy. *In* Biological Membranes. A Molecular Perspective from Computation and Experiment. J. Merz and B. Roux, editors. Birkhäuser, Basel. 175–252.

Büldt, G., H. U. Galley, A. Seelig, J. Seelig, and G. Zacci. 1978. Neutron diffraction studies on selectively deuterated phospholipid bilayers. *Nature.* 271:182–184.

Crilly, J. F., and J. C. Earnshaw. 1983a. Cholesterol-induced effects on the viscoelasticity of monoglyceride bilayers. *Biophys. J.* 41:211–216.

Crilly, J. F., and J. C. Earnshaw. 1983b. Photon correlation spectroscopy of bilayer lipid membranes. *Biophys. J.* 41:197–210.

Crilly, J. F., and J. C. Earnshaw. 1985. Light scattering from fluid interfaces: considerations of some instrumental effects. *J. Phys. D.* 18:609–616.

Diederich, A., C. Hödl, D. Pum, U. B. Sleytr, and M. Lösche. 1996. Reciprocal influence between the protein and lipid components of a lipid-protein membrane model. *Colloids Surf., B.* 6:335–343.

Fan, C. 1973. Fluctuations and light scattering from anisotropic interfaces. *J. Colloid Interface Sci.* 44:369–381.

Grabowski, E. F., and J. A. Cowen. 1977. Thermal excitations of a bilipid membrane. *Biophys. J.* 18:23–28.

Györvary, E., B. Wetzer, U. B. Sleytr, A. Sinner, A. Offenhäusser, and W. Knoll. 1999. Lateral diffusion of lipids in silane-, dextran-, and S-layer-supported mono and bilayers. *Langmuir.* 15:1337–1347.

Helfrich, W., and R. M. Servuss. 1984. Undulations, steric interaction and cohesion of fluid membranes. *Il Nuovo Cimento.* 3:137–151.

Hirn, R., T. M. Bayerl, J. O. Rädler, and E. Sackmann. 1999a. Collective membrane motions of high and low amplitude studied by dynamic light scattering and microinterferometry. *JCS Faraday Trans. II.* 111:17–30.

Hirn, R., R. Benz, and T. M. Bayerl. 1999b. Collective membrane motions in the mesoscopic range and their modulation by the binding of a mono-molecular protein layer of streptavidin. *Phys. Rev. E.* 59: 5987–5994.

König, H. 1988. Archaebacterial cell envelopes. *Can. J. Microbiol.* 34: 305–406.

Kramer, L. 1971. Theory of light scattering from fluctuations of membranes and monolayers. *J. Chem. Phys.* 55:2097–2105.

Linseisen, F. M., S. Bayerl, and T. M. Bayerl. 1996. 2H-NMR and DSC study of DPPC-DODAB mixtures. *Chem. Phys. Lipids.* 83:9–23.

Lipowsky, R. 1996. Generic interactions of flexible membranes. *In* Structure and Dynamics of Membranes. R. Lipowsky and E. Sackmann, editors. Elsevier Science B. V., Amsterdam. 521–602.

MacDonald, P. M., J. Leisen, and F. M. Marassi. 1991. Response of phosphatidylcholine in the gel and liquid-crystalline states to membrane surface charges. *Biochemistry.* 30:3558–3566.

Pfeiffer, W., S. König, J. F. Legrand, T. M. Bayerl, D. Richter, and E. Sackmann. 1993. Neutron spin echo study of membrane undulations in lipid multibilayers. *Europhys. Lett.* 23:457–462.

Pum, D., and U. B. Sleytr. 1994. Large-scale reconstitution of crystalline bacterial surface layer proteins at the air-water interface and on lipid films. *Thin Solid Films.* 244:882–886.

Pum, D., and U. B. Sleytr. 1996. Molecular nanotechnology and biomimetics with S-layers. *In* Crystalline Bacterial Cell Surface Proteins. U. B. Sleytr, P. Messner, D. Pum, and M. Sára, editors. Academic Press, New York. 175–209.

Pum, D., M. Weinhandel, C. Hödl, and U. B. Sleytr. 1993. Large-scale recrystallization of the S-layer of *Bacillus coagulans* E38-66 at the air/water interface and on lipid films. *J. Bacteriol.* 175:2762–2766.

Sackmann, E. 1996. Physical basis of self-organization and function of membranes: physics of vesicles. *In* Structure and Dynamics of Membranes. R. Lipowsky and E. Sackmann, editors. Elsevier Science B. V., Amsterdam. 213–304.

Sára, M., D. Pum, and U. B. Sleytr. 1992. Permeability and charge-dependent adsorption properties of the S-layer lattice from *Bacillus coagulans* E38-66. *J. Bacteriol.* 174:3487–3493.

Sára, M., and U. B. Sleytr. 1993. Relevance of charged groups for the integrity of the S-layer from *Bacillus coagulans* E38-66 and for molecular interactions. *J. Bacteriol.* 175:2248–2254.

Schuster, B., D. Pum, O. Braha, H. Bayley, and U. B. Sleytr. 1998a. Self-assembled a-hemolysin pores in an S-layer-supported lipid bilayer. *Biochim. Biophys. Acta.* 1370:280–288.

Schuster, B., D. Pum, and U. B. Sleytr. 1998b. Voltage clamp studies on S-layer-supported tetraether lipid membranes. *Biochim Biophys Acta.* 1369:51–60.

Seifert, U., and S. A. Langer. 1993. Viscous modes of fluid bilayer membranes. *Europhys. Lett.* 23:71–76.

Sleytr, U. B., and P. Messner. 1989. Self-assembly of crystalline bacterial cell surface layers (S-layers). *In* Electron Microscopy of Subcellular Dynamics. H. Plattner, editor. CRC Press, Boca Raton. 13–31.

Sleytr, U. B., P. Messner, D. Pum, and M. Sára. 1996a. Occurrence, location, ultrastructure and morphogenesis of S-layers. *In* Crystalline Bacterial Cell Surface Protein. U. B. Sleytr, P. Messner, D. Pum, and M. Sára, editors. Academic Press, Austin, Texas. 5–34.

Sleytr, U. B., M. Sára, Z. Küpcü, and P. Messner. 1996b. Structural and chemical characterization of S-layers of selected strains of *Bacillus stearothermophilus* and *Desulfotomaculum nigrificans. Arch. Microbiol.* 146:19–24.

Stohrer, J., G. Gröbner, D. Reimer, K. Weisz, C. Mayer, and G. Kothe. 1991. Collective lipid motions in bilayer membranes studied by transverse deuteron spin relaxation. *J. Chem. Phys.* 95:672–678.

Vrij, A., J. G. H. Joosten, and H. M. Fijnaut. 1981. Light scattering from thin liquid films. *In* Advances in Chemical Physics. I. Prigogine and S. A. Rice, editors. John Wiley and Sons, Inc. New York. 330–396.

Wetzer, B., A. Pfandler, E. Györvary, D. Pum, M. Lösche, and U. B. Sleytr. 1998. S-layer reconstitution at phospholipid monolayers. *Langmuir.* 14:6899–6906.

Weygand, M., B. Wetzer, D. Pum, U. B. Sleytr, N. Cuvillier, K. Kjaer, P. B. Howes, and M. Lösche. 1999. Bacterial S-layer protein coupling to lipids: x-ray reflectivity and grazing incidence diffraction studies. *Biophys. J.* 76:458–468.

Zilker, A., H. Engelhardt, and E. Sackmann. 1987. Dynamic reflection interference contrast (RIC-) microscopy: a new method to study surface excitations of cells and to measure membrane bending elastic moduli. *J. Phys. (France).* 48:2139–2151.